International Journal of Engineering Trends and Technology
ISSN: 2231–5381 / https://doi.org/10.14445/22315381/IJETT-V72I11P103

Volume 72 Issue 11, 16-22, November 2024

Original Article

A Study on the Design of High-Speed Shaft Coupling for a 6MW Wind Turbine

Dong-Seuk Oh[1], Young-Kuk Kim[1], Yu-Jin Jeong[1], Min-Woo Kim[1], Jong-Hun Kang[2], Hyoung-Woo Lee[2*]

[1]*Department of Mechanical Engineering, Jungwon University, Republic of Korea, Chungbuk.*
[2]*Department of Unmanned Aeromechanical Engineering, Jungwon University, Republic of Korea, Chungbuk.*

[*]*Corresponding Author : leehwoo@jwu.ac.kr*

Received: 09 September 2024 Revised: 07 November 2024 Accepted: 13 November 2024 Published: 29 November 2025

Abstract *- The high-speed shaft coupling is a critical component of the power transmission system, with its safety and durability directly impacting the overall system's stability. Traditional manufacturing methods for high-speed shaft couplings primarily involve bonding fiberglass spacers to the flange. However, there have been instances where parts of the bonded spacer detach from the lower part of the flange, potentially leading to coupling failure. This issue can result in equipment downtime and reduced safety. In this study, we propose a method to reinforce the spacer by inserting pins, aiming to improve the safety of the high-speed shaft coupling. Through structural and fatigue analyses, we verify whether this approach can maintain structural stability even if part of the bonded spacer detaches. The findings of this study are expected to enhance the reliability of high-speed shaft couplings for 6MW wind turbines and contribute to securing the long-term operational safety of the equipment.*

Keywords *- Wind-turbine, High-speed shaft coupling, Tsai-Wu, Orthotropic anisotropy, Palmgren miner's rule.*

1. Introduction

Wind power generation has emerged as a key technology for environmentally friendly energy production, with significant advancements in developing large-scale wind turbines. Within the power transmission system of such turbines, high-speed shaft coupling is a critical component that influences the stability and performance of the overall system. Its reliability is directly linked to the operational safety of the entire wind turbine. Traditional manufacturing methods for high-speed shaft couplings primarily involve using fiberglass spacers bonded to the flange. However, issues have been reported regarding parts of these bonded spacers becoming detached.

This detachment primarily occurs due to debonding between the spacer and flange, which can exacerbate the risk of coupling failure. Such detachment can lead to the failure of the high-speed shaft coupling, resulting in turbine downtime and severe safety concerns. Particularly in large-scale 6MW wind turbines, this issue can cause economic losses and negatively impact the stability of the energy supply [1]. As such, it is essential to research the reinforcement of high-speed shaft coupling spacers in wind turbines. Researchers have employed various approaches in the study of high-speed shaft couplings. For instance, H.W. Lee and J.H. Kang conducted Finite Element Analysis (FEA) to ensure the structural stability of high-speed shaft couplings and analyzed their structural performance. To extend the fatigue life of wind turbine high-speed shaft couplings, selecting materials and applying safety factors during the design process are critical. According to the IEC 61400-1 standard, wind turbine components must be designed with a safety factor of at least 1.3, which is crucial for extending the fatigue life of couplings [2]. To visually clarify the overall reinforcement process of the coupling spacers, a flow chart is presented in Figure 1.

Fig. 1 Coupling spacer reinforcement process procedure

In this study, we propose a new method of reinforcing the spacers by inserting pins, in addition to the traditional bonding method. There have been no documented cases of reinforcement between flanges and composite spacers using pins, and there is a lack of verification regarding the impact of this reinforcement method on structural safety. Aim to verify, through structural and fatigue analyses, whether this reinforcement method can improve structural safety. Specifically, this paper examines whether the high-speed shaft coupling components for wind turbines are designed to meet the target safety factor of 1.3, as recommended in IEC 61400-1. The Tsai-Wu criterion is applied to assess structural stability through structural analysis for fibreglass spacers. In addition, fatigue analysis will verify the performance under Load Duration Distribution (LDD) loads and Markov Matrix conditions for wind turbines.

2. Structural Analysis of High Speed Coupling

2.1. Finite Element Analysis Overview

As shown in Figure 2, instead of analyzing the full model of the high-speed shaft coupling, a simplified model consisting of the flange, spacer, and pins, which are the areas of interest, was used for finite element analysis. This simplified model was designed to accurately analyze the stress concentration and contact conditions occurring within the system. Only the flange section where actual coupling occurs was considered, with the model consisting of the spacer, flange, and pin. During the modeling process, appropriate contact and boundary conditions between the components were set, with the primary goal of the analysis being to precisely identify stress concentrations in specific areas and evaluate the structural stability based on these results.

Developed using ANSYS 2024 R1, the finite element model consists of 350,144 nodes and 270,945 elements. A hex-dominant, multizone method was applied for meshing with 10mm and 5mm mesh sizes. The pin insertion area was modeled with an edge size of 2mm to enhance accuracy. Additionally, the spacer was modeled using shell elements to accurately represent the Tsai-Wu criterion, with the spacer being composed of layers of orthotropic anisotropic material [3].

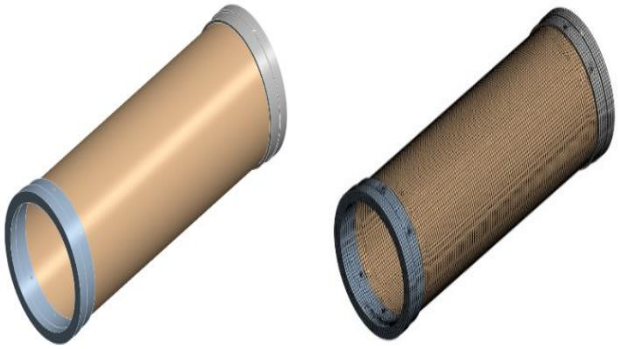

Fig. 2 Finite element analysis model of high-speed shaft coupling for wind turbines

2.2. Material Properties for Finite Element Analysis

The spacer made of GFRP (Glass Fiber Reinforced Plastics) has the material properties shown in Table 1. Equivalent material properties considering orthotropic anisotropy were obtained through actual tensile and bending tests and then layered using ANSYS ACP. Applying orthotropic GFRP enhanced the efficiency of the design by increasing strength and stiffness [4]. The spacer has a thickness of 8mm, and the actual stacking angle of 54.8 degrees was applied to accurately reflect the composite material layers' characteristics.

Figure 3 illustrates this laminated structure, clearly demonstrating the properties of an orthotropic anisotropic material. Specifically, as shown in Figure 4, the orthotropic nature of the material can be visually verified through Elemental Triads in ANSYS, which show how each fiber layer is arranged. Elemental Triads are used to confirm that the material's coordinate system is correctly defined in a cylindrical coordinate system, ensuring that the orthotropic anisotropic properties of the spacer are accurately represented within the cylindrical structure. This setting is essential for accurately simulating the actual operating environment of the high-speed shaft coupling.

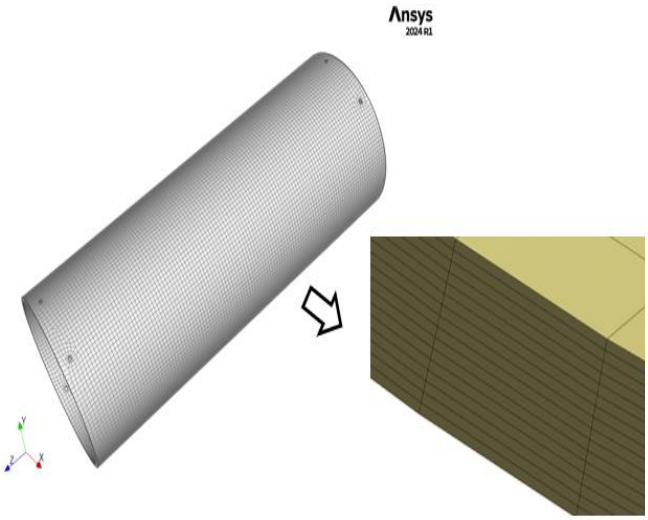

Fig. 3 ACP module laminate

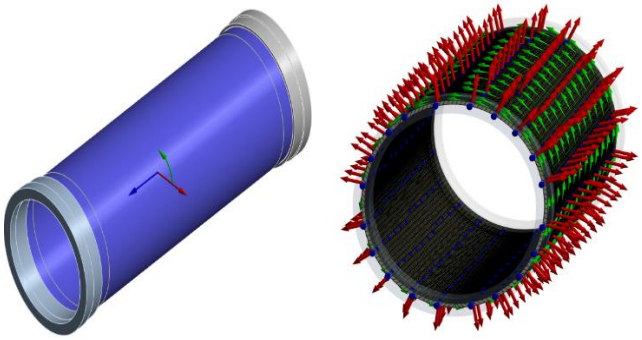

Fig. 4 (r, θ, z)Orthotropic anisotropy

Table 1. Material properties of the spacer of the high-speed shaft coupling

Properties	Symbol	Unit	Value
Elastic Modulus	E1	GPa	43.4
	E2	GPa	12.1
	E3	GPa	12.1
Poisson's Ratio	v12		0.294
	v23		0.294
	v13		0.294
Shear Modulus	G12	GPa	4.64
	G23	GPa	4.68
	G13	GPa	4.64

2.3. Boundary Conditions

Considering the possibility of spacer bonding failure and the pin insertion method, multiple cases were established for boundary conditions, as shown in Figure 5. The load value was set to a torque of 86,000Nm. This torque value was selected as the slip torque, representing the threshold at which relative rotation may begin between the coupled components. In Figure 6, Case 1 only considers bonding, while Case 2 considers both bonding and the inserted pin. In Case 2, a bolt-joining method is applied alongside boding to enhance structural stability, strengthening the robustness of the connection. This combined approach increases the durability of the joint, ensuring it maintains stability against external impacts. These cases provide a comparison standard for evaluating the coupling's performance under optimal conditions. Figure 7 shows Case 3, where the boundary conditions simulate the detachment of a significant portion of the spacer. The analysis focuses on areas where detachment has been reported, and it verifies whether the inserted pin can prevent or mitigate structural issues.

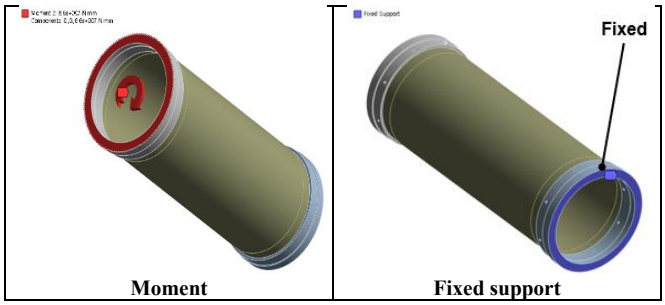

Fig. 5 Boundary conditions of all cases

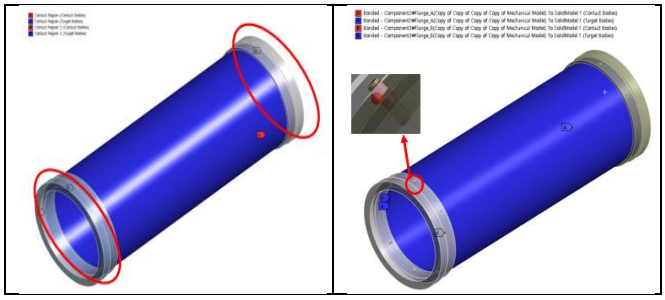

Fig. 6 Boundary conditions of Case 1,2

Fig. 7 Boundary conditions of Case 3

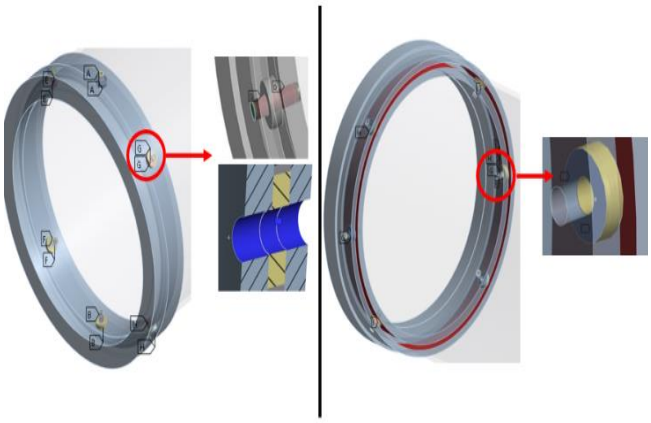

Fig. 8 Boundary conditions of Case 4,5

Figure 8 shows Cases 4 and 5, which simulate bonding failure around the pin, assessing the potential for stress concentration around the pin to lead to structural degradation. Boundary conditions were set to simulate realistic scenarios, such as the displaced pin or stress concentrations forming around it. The friction coefficient was set to 0.3 to accurately reflect actual conditions that could occur in mechanical contact scenarios like those in the coupling. The friction coefficient is critical in ensuring accurate load transfer between components in cases where bonding is partially or entirely compromised. A comprehensive analysis was conducted for these five cases, and non-linear analysis was selected to perform the simulations.

2.4. Analysis Results

Based on the finite element analysis, a total of five simulation cases were performed, combining various structural configurations involving the flange, spacer, and pin. The equivalent stress of the flange was analyzed for each case, with comparisons made against the material's yield criteria to evaluate safety. In all cases, the safety factor exceeds 1.35, as recommended for wind turbine components in IEC 61400-1, confirming the safety of the design. For the spacer, the

principal stress was assessed with respect to the Tsai-Wu criterion, considering the characteristics of the composite material and fatigue analysis to evaluate the possibility of failure. In addition, the safety factor was compared to assess the structural safety following the pin insertion. The results of these cases are summarized in Tables 2 and 3.

Table 2. High-speed shaft coupling stress result

Case	Value	Spacer	Flange A	Flange B
		Principal Stress	Equivalent Stress	Equivalent Stress
1	86kNm	74.26	234.37	268.42
2		79.19	292.12	322.63
3		86.85	377.86	370.71
4		114.21	340.68	325.53
5		118.75	463.84	284.52

Table 3. High-speed shaft coupling safety factor

Case	Value	Flange A	Flange B
1	86kNm	3.56	3.11
2		2.86	2.59
3		2.21	2.25
4		2.45	2.57
5		1.80	2.93

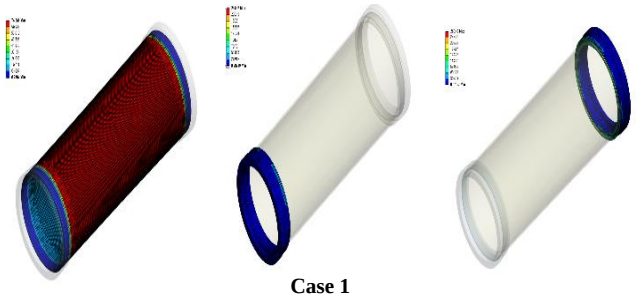

Case 1

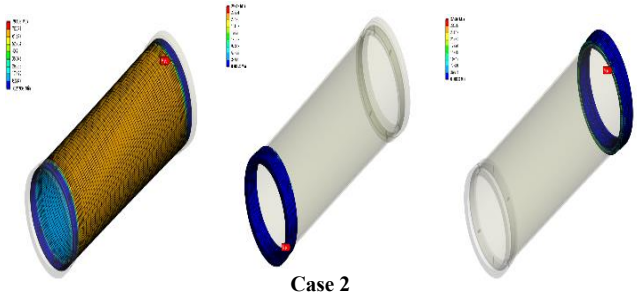

Case 2

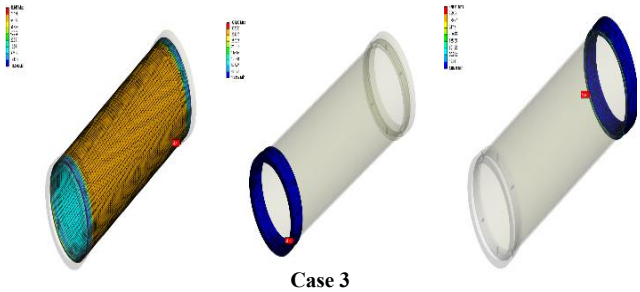

Case 3

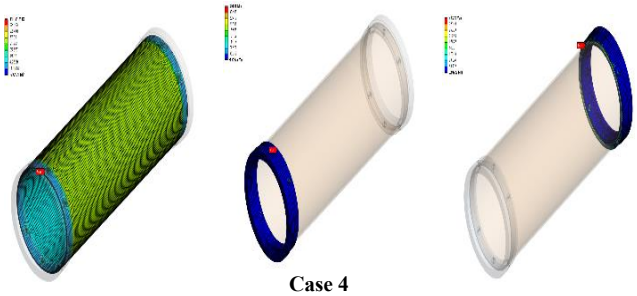

Case 4

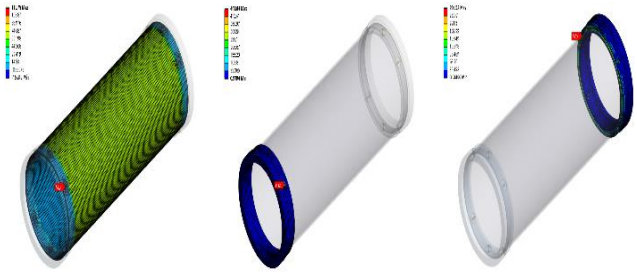

Case 5

Fig. 9 High-speed shaft coupling stress analysis result

In Case 1, where only bonding was applied, the stress distribution of flange A, flange B, and the spacer was analyzed. The stresses at flange A and B were found to be 234.37 MPa and 268.42 MPa, respectively, with maximum stress occurring at these points. The maximum principal stress in the spacer was 74.26 MPa. These stress values were within the allowable design limits, confirming that bonding alone provided sufficient safety. In Case 2, where bonding and pin insertion were applied, the maximum stresses at flange A and B were 292.12 MPa and 322.63 MPa, respectively. The stress in the spacer was 79.19 MPa. Although the stress values were slightly increased, they were still within the allowable design range, confirming that the combined application of bonding and pin insertion posed no structural safety concerns. In Case 3, which applied friction conditions and pin insertion to the area where bonding had failed, the stress increased significantly. The results showed 377.86 MPa and 370.71 MPa at flange A and B, respectively, while the spacer experienced a stress of 86.85 MPa. The significant increase in stress was attributed to a stress concentration around the pin due to the bonding failure, suggesting that bonding failure can lead to structural vulnerabilities and highlighting the importance of pin insertion. In Case 4, which simulated bonding failure within a 30mm radius around the pin and applied friction conditions between the spacer and the pin, the stress was reduced compared to Case 3. However, stress concentration still occurs in the spacer, made of orthotropic anisotropic material, indicating that special attention is needed in this area. In Case 5, where the bonding failure radius around the pin was increased by 10mm compared to Case 4, the highest maximum stress was observed in the flange, and the stress in the spacer was also higher than in Case 4. This indicates that as the bonding failure area increases, structural stability weakens. However, safety was maintained under

extreme conditions. The Tsai-Wu failure criterion was used separately from the fatigue damage calculation to evaluate the failure potential of the composite spacer. Since the material and structural characteristics differ from isotropic materials like metals, the Tsai-Wu Strength Index was used to judge failure rather than the safety factor, and it was derived using the following formula. It simultaneously reflects the stress states of tension, compression, and shear within the material.

$$F_1\sigma_1 + F_2\sigma_2 + F_3\sigma_3 + F_4\sigma_4 + F_5\sigma_5 + F_6\sigma_6 + F_{11}{\sigma^2}_1 + F_{22}{\sigma^2}_2 + F_{33}{\sigma^2}_3 + F_{44}{\sigma^2}_4 + F_{55}{\sigma^2}_5 + F_{66}{\sigma^2}_6 + 2F_{12}\sigma_1\sigma_2 + 2F_{13}\sigma_1\sigma_3 + 2F_{23}\sigma_2\sigma_3 \leq 1 \quad Eq.(1)$$

The Tsai-Wu Strength Index was calculated using ANSYS 2024 R1's APDL, and the results are shown in Table 4 and Figure 10.

Table 4. Tsai-Wu strength index result

Case	Value	Spacer	Thickness[mm]
			8
1	86kNm	Tsai-Wu Strength Index	0.32
2			0.34
3			0.58
4			0.45
5			0.48

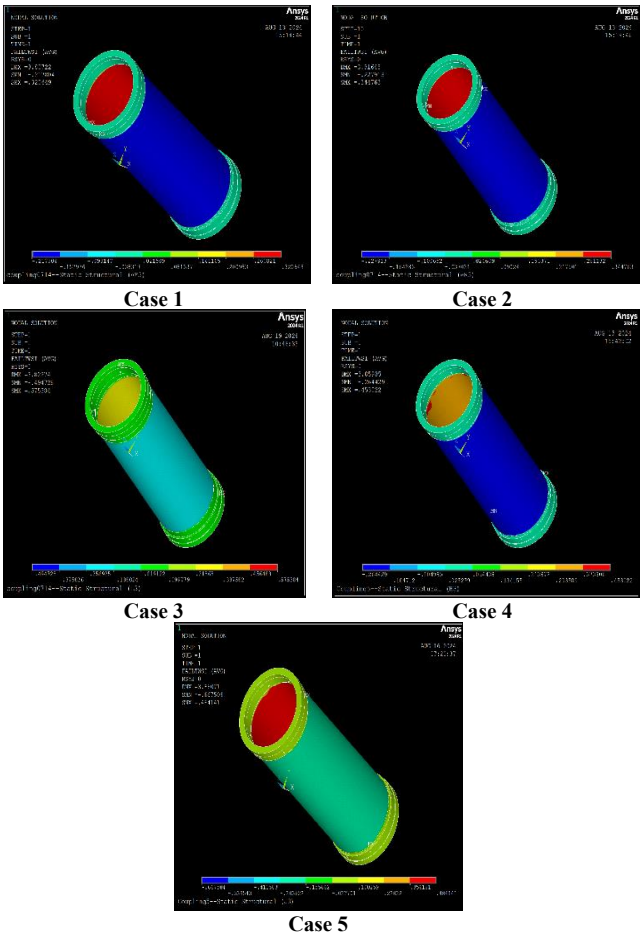

Fig. 10 High-speed shaft coupling Tsai-Wu strength index result

In Case 1, using the traditional bonding method, the analysis showed a Tsai-Wu Strength Index of 0.32, indicating a very low probability of failure. On the other hand, in Case 2, although there was some stress concentration due to the insertion of the pin, the Tsai-Wu Strength Index was 0.34, which is still within the safe range. This suggests that pin insertion does not significantly affect structural safety. In Case 3, despite the stress concentration caused by bonding failure, the Tsai-Wu Strength Index increased to 0.58. Although slightly higher, this value still indicates a low risk of failure, demonstrating that pin insertion can ensure a certain level of safety even in bonding failure scenarios. In Case 4 and Case 5, the Tsai-Wu Strength Index values were 0.45 and 0.48, respectively. These results show that the probability of failure remains low even when bonding has failed, and stress concentration occurs around the pin. In particular, the risk of failure does not significantly increase compared to cases without pin insertion. Therefore, it is evident that even if partial bonding failure occurs in high-speed shaft coupling, pin insertion can maintain sufficient structural safety.

3. Fatigue Analysis

The rotational motion of the high-speed shaft coupling generates significant torque, and continuous operation leads to accumulated fatigue. To maintain the long-term stability of wind turbines, it is essential to evaluate this fatigue accumulation accurately. Using LDD (Load Duration Distribution) data from the wind turbine, the fatigue accumulation was assessed using a Markov matrix. The LDD data represents the various load conditions experienced over time in a wind turbine, and from this, a Markov matrix was constructed to represent the transition probabilities between states. Figure 11 shows the Markov matrix as a matrix of transition probabilities between states, which is used to predict how fatigue damage accumulates over time as load states change. The fatigue accumulation values derived from this study were combined with the structural analysis results to perform a fatigue analysis. Palmgren-Miner's Rule was applied to calculate fatigue damage using the stress distribution from the structural analysis and the transition probabilities predicted by the Markov matrix.

The formula for Miner's rule is shown in Equation (2). For the SCM440 flange, equivalent stress was applied, while for the GFRP composite spacer, maximum principal stress was used as it is more prone to damage in specific stress directions.

$$D = \sum \frac{n_{Ei}}{N_{Ri}} \leq 1 \qquad (2)$$

The results are summarized in Table 5, and these fatigue analysis results play a critical role in evaluating the long-term reliability of the wind turbine's high-speed shaft coupling. By predicting potential fatigue damage under various operating conditions, design improvements can be proposed to extend the coupling's design life and prevent unexpected failures. The SN curves for each component are shown in Figures 12 and

13, where the Safe Life method, as specified in Eurocode 3 (EN 1993-1-9), was applied to ensure safety and to calculate the cumulative fatigue damage of the wind turbine components [5]. Fatigue damage exceeding 1 is considered as exceeding the fatigue limit.

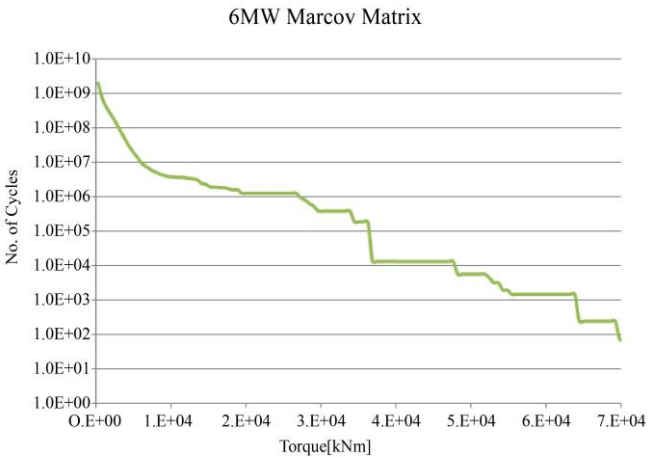

Fig. 11 6MW class wind turbine Markov matrix

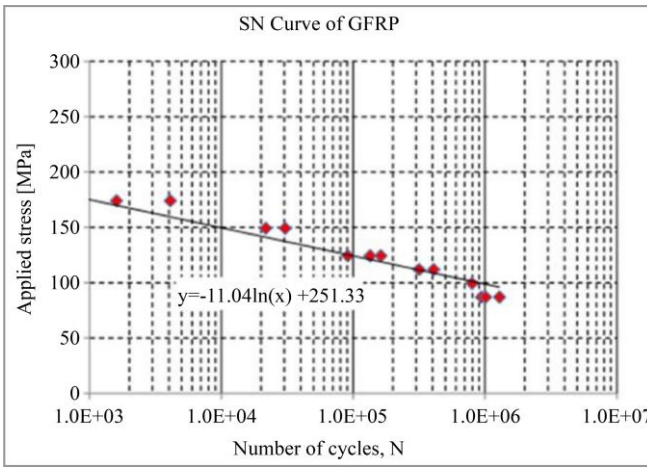

Fig. 12 GFRP S-N curve

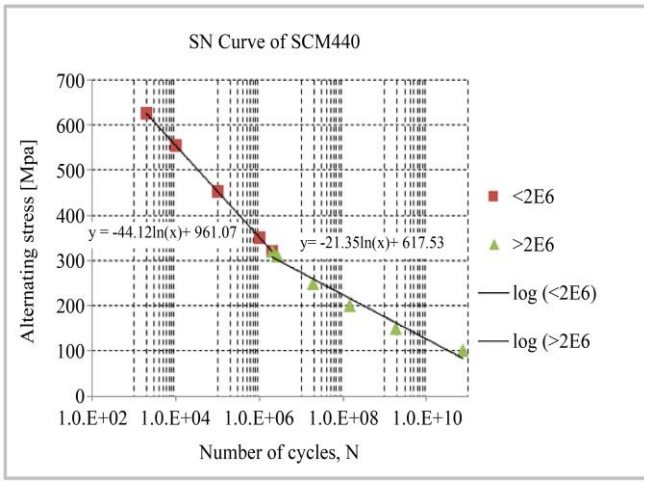

Fig. 13 SCM440 S-N curve

Table 5. High-speed shaft coupling fatigue damage results

		Flange B
Case 1	Flange	0.003
	Spacer	0.592
Case 2	Flange	0.011
	Spacer	0.611
Case 3	Flange	0.038
	Spacer	0.647
Case 4	Flange	0.016
	Spacer	0.904
Case 5	Flange	0.141
	Spacer	0.983

In Case 1, where the spacer was bonded, the stability of the fatigue analysis was confirmed. In Case 2, where the spacer was bonded, and pins were inserted, the pins prevented the fiberglass spacer from tearing. In Case 3, sufficient safety was also demonstrated when friction was applied to the spacer's edge. For Cases 4 and 5, where the bonding was absent within a 30 mm and 40 mm radius around each of the 12 pins and friction was applied to the pins, tears were not observed in the fiberglass spacer, similar to the previous cases. Overall, the structural performance remained stable.

4. Conclusion

In this study, a pin insertion method was applied to improve the structural safety of the high-speed shaft coupling and analyze the potential failure caused by bonding detachment. Various simulation cases confirmed that pin insertion can provide sufficient structural stability even in situations where partial bonding detachment occurs. The Tsai-Wu Strength Index evaluation demonstrated that the combined application of bonding and pin insertion significantly enhances structural stability, ensuring that the coupling maintains its integrity under operational stresses. Specifically, the Tsai-Wu Strength Index values across different cases indicated that the risk of failure is minimized, with the index remaining within safe limits. Furthermore, the stability of the flange was also confirmed through equivalent stress analysis, which showed that the stress levels in the flange remained well within the material's yield limits across all cases. This finding indicates that the flange and the spacer maintain their structural safety under expected loading conditions. The evaluation using the Tsai-Wu Strength Index indicated that when bonding and pin insertion are combined, the likelihood of coupling failure remains low, and pin insertion alone can effectively reinforce structural safety.

In particular, the Tsai-Wu strength Index for pins in Cases 4 and 5, where stress concentration was anticipated, remained at safe levels of 0.45 and 0.48, respectively. Case 3, which involved actual bonding detachment, also showed a safe Tsai-Wu Strength Index of detachment and a safe Tsai-Wu Strength Index of 0.58, confirming the structural reliability even under these conditions. These research findings suggest that incorporating pin insertion in the design of high-speed shaft

couplings can reduce the potential risks associated with bonding detachment. This method can be particularly valuable in large systems, such as wind turbines, by enhancing the reliability of couplings. It is thus expected to continuously improve the design and operational stability of high-speed shaft couplings.

References

[1] IEC 61400-1:2019, Wind Energy Generation Systems - Part 1: Design Requirements, 2019. [Online]. Available: webstore.iec.ch/en/publication/26423.

[2] Le Ling, Yan Li, and Sicheng Fu, "A Reliability Analysis Strategy for Main Shaft of Wind Turbine Using Importance Sampling and Kriging Model," *International Journal of Structural Integrity*, vol. 13, no. 2, pp. 297-308, 2022. [CrossRef] [Google Scholar] [Publisher Link]

[3] Jin-Ah Lee et al., "Design of Composite Laminate Bicycle Wheel considering Stacking Sequence," *The Korean Society for Composite Materials (KSM)*, vol. 25, no. 5, pp. 141-146, 2012. [CrossRef] [Google Scholar] [Publisher Link]

[4] Kim Jin-Sung, Roh Jin-Ho, and Lee Soo-Yong, "Failure Prediction for Composite Materials under Flexural Loading," *The Korean Society for Aeronautical and Space Sciences*, vol. 45, no. 12, pp.1013-1020, 2017. [CrossRef] [Google Scholar] [Publisher Link]

[5] BS EN 1993-1-2:2005, Eurocode 3. Design of Steel Structures - General Rules - Structural Fire Design, 2005. [Online]. Available: https://knowledge.bsigroup.com/products/eurocode-3-design-of-steel-structures-general-rules-structural-fire-design?version=standard